DOI:
10.1172/jci.insight.134310

JCI insight

Requirement of FAT and DCHS protocadherins during hypothalamic-pituitary development

Emily J. Lodge, … , Constantine Stratakis, Cynthia L. Andoniadou

JCI Insight. 2020. https://doi.org/10.1172/jci.insight.134310.

Research In-Press Preview **Development** **Endocrinology**

Pituitary developmental defects lead to partial or complete hormone deficiency and significant health problems. The majority of cases are sporadic and of unknown cause. We screened 28 patients with pituitary stalk interruption syndrome (PSIS) for mutations in the FAT/DCHS family of protocadherins that have high functional redundancy. We identified seven variants, four of which putatively damaging, in *FAT2* and *DCHS2* in six patients with pituitary developmental defects recruited through a cohort of patients with mostly ectopic posterior pituitary gland and/or pituitary stalk interruption. All patients had growth hormone deficiency and two presented with multiple hormone deficiencies and small glands. FAT2 and DCHS2 were strongly expressed in the mesenchyme surrounding the normal developing human pituitary. We analyzed *Dchs2*$^{-/-}$ mouse mutants and identified anterior pituitary hypoplasia and partially penetrant infundibular defects. Overlapping infundibular abnormalities and distinct anterior pituitary morphogenesis defects were observed in *Fat4*$^{-/-}$ and *Dchs1*$^{-/-}$ mouse mutants but all animal models displayed normal commitment to the anterior pituitary cell type. Together our data implicate FAT/DCHS protocadherins in normal hypothalamic-pituitary development and identify *FAT2* and *DCHS2* as candidates underlying pituitary gland developmental defects such as ectopic pituitary gland and/or pituitary stalk interruption.

Requirement of FAT and DCHS protocadherins during hypothalamic-pituitary development

Emily J. Lodge[1,*], Paraskevi Xekouki[1,2,*], Tatiane S. Silva[3], Cristiane Kochi[3], Carlos A. Longui[3], Fabio R. Faucz[4], Alice Santambrogio[1,5], James L. Mills[6], Nathan Pankratz[7], John Lane[7], Dominika Sosnowska[1], Tina Hodgson[1], Amanda L. Patist[1], Philippa Francis-West[1], Françoise Helmbacher[8], Constantine A. Stratakis[4], Cynthia L. Andoniadou[1,5]

[1]Centre for Craniofacial and Regenerative Biology, King's College London, Floor 27 Tower Wing, Guy's Campus, London, SE1 9RT, United Kingdom
[2]Current address: Endocrinology and Diabetes Clinic, University General Hospital of Heraklion, University of Crete Medical School, Heraklion Crete, 71003, Greece
[3]Pediatric Endocrinology Unit, Irmandade da Santa Casa de Misericórdia de São Paulo, São Paulo, Brazil.
[4]Section on Endocrinology and Genetics, *Eunice Kennedy Shriver* National Institute of Child Health and Human Development, National Institutes of Health (NIH), Bethesda, Maryland
[5]Department of Medicine III, University Hospital Carl Gustav Carus, Technische Universität Dresden, Dresden 01307, Germany
[6]Division of Intramural Population Health Research, Epidemiology Branch, Eunice Kennedy Shriver National Institute of Child Health and Human Development (NICHD), National Institutes of Health (NIH), Bethesda, Maryland, USA
[7]Department of Laboratory Medicine and Pathology, University of Minnesota Medical School, Minneapolis, Minnesota, USA
[8]Aix Marseille Université, CNRS, IBDM - UMR7288, Marseille, France.
* These authors contributed equally to this work

Correspondence: Cynthia L. Andoniadou
Address: Centre for Craniofacial and Regenerative Biology, King's College London, Floor 27 Tower Wing, Guy's Campus, London, SE1 9RT, United Kingdom
Tel +44 207 188 7389
Fax +44 207 188 1674
Email : cynthia.andoniadou@kcl.ac.uk

The authors have declared that no conflict of interest exists.

Abstract

Pituitary developmental defects lead to partial or complete hormone deficiency and significant health problems. The majority of cases are sporadic and of unknown cause. We screened 28 patients with pituitary stalk interruption syndrome (PSIS) for mutations in the FAT/DCHS family of protocadherins that have high functional redundancy. We identified seven variants, four of which putatively damaging, in *FAT2* and *DCHS2* in six patients with pituitary developmental defects recruited through a cohort of patients with mostly ectopic posterior pituitary gland and/or pituitary stalk interruption. All patients had growth hormone deficiency and two presented with multiple hormone deficiencies and small glands. FAT2 and DCHS2 were strongly expressed in the mesenchyme surrounding the normal developing human pituitary. We analyzed *Dchs2*$^{-/-}$ mouse mutants and identified anterior pituitary hypoplasia and partially penetrant infundibular defects. Overlapping infundibular abnormalities and distinct anterior pituitary morphogenesis defects were observed in *Fat4*$^{-/-}$ and *Dchs1*$^{-/-}$ mouse mutants but all animal models displayed normal commitment to the anterior pituitary cell type. Together our data implicate FAT/DCHS protocadherins in normal hypothalamic-pituitary development and identify *FAT2* and *DCHS2* as candidates underlying pituitary gland developmental defects such as ectopic pituitary gland and/or pituitary stalk interruption.

Introduction

Developmental pituitary defects affect 0.5 in 100,000 live births and may lead to varying degrees of pituitary hormone deficiency (1, 2). Beyond biochemical confirmation of hormonal defects, diagnosis is based on magnetic resonance imaging (MRI) to identify a small or absent anterior pituitary, interrupted or absent pituitary stalk (pituitary stalk interruption syndrome or PSIS) and ectopic posterior pituitary (EPP) (3).

During embryonic development, a region of the ventral diencephalon of the hypothalamus termed the infundibulum, and a region of the oral epithelium termed Rathke's pouch (RP), evaginate towards each other to form the pituitary gland. These actions are mediated by an array of developmental signals as well as the action of the surrounding mesenchyme (for review see (4)). RP gives rise to the anterior pituitary whilst the infundibulum gives rise to the posterior pituitary and the pituitary stalk, which connects the posterior lobe to the hypothalamus. The vast majority of cases with pituitary developmental defects are sporadic and of unknown cause; few cases appear to be familial and they are often attributed to germline biallelic mutations in transcription factors involved in the development of the infundibulum (5-7). Recently a whole exome sequencing (WES) screen of patients with such defects identified compound defects in *DCHS1* among other gene variants, indicating that protocadherins could be involved in pituitary development (8).

Cadherins represent a major family of adhesion molecules involved in tissue formation. As such they possess extracellular domains which facilitate binding, as well as an intracellular domain capable of associating with adaptor and signaling proteins (9). FAT and DCHS protocadherins act as ligand-receptor pairs when expressed in adjacent cells and have

been implicated both in planar cell polarity (PCP) regulating cell movements such as convergence-extension and cell migration (10, 11), as well as regulation of YAP/TAZ independently of the Hippo kinase cascade (12-14), which controls tissue proliferation and stem cell activity (15).

In humans there are four *FAT* paralogues (*FAT1*, *FAT2*, *FAT3* and *FAT4*) and two *DCHS* paralogues (*DCHS1* and *DCHS2*) (16). Mutations in *FAT4* are linked to Hennekam syndrome, whilst biallelic mutations in *FAT4* or *DCHS1* genes are associated with Van Maldergem syndrome (VMS). Besides symptoms common to both syndromes, such as intellectual disability and craniofacial malformations, VMS-specific clinical symptoms additionally include camptodactyly, syndactyly, small kidneys, osteopenia and tracheal abnormalities (14, 17-21), whereas lymphangiectasia and lymphedema are specific to Hennekam syndrome (17, 18, 22). A link between VMS and endocrine abnormalities including hypogonadotropic hypogonadism and amazia, were reported in a recent study, providing new support to the possible involvement of FAT/DCHS signaling in hypothalamic-pituitary axis development or function (23). Null deletions of *Fat4* or *Dchs1* in mouse lead to overlapping phenotypes, including inner ear, neural tube, kidney, skeleton, lung, and heart defects (24) further supporting that these protocadherins act as a ligand-receptor pair. However, both mutant mice die shortly after birth, inhibiting the study of postnatal homozygous null animals (24, 25). *Dchs2*$^{-/-}$ mutant mice are viable and fertile, with analyses revealing functional redundancy between DCHS2 and DCHS1 (26). DCHS1 exhibits a broader expression pattern during development and its loss generally results in more severe developmental phenotypes (16). We have previously characterized expression patterns of *Dchs1*, *Fat3* and *Fat4* during murine embryonic development and identified expression in the hypothalamus, infundibulum, developing RP and surrounding mesenchyme (27).

In this study we performed WES on 28 patients with EPP and/or PSIS and identified variants in *FAT2* and *DCHS2* predicted to be deleterious. We characterized expression of FAT2 and DCHS2 in the human developing gland and analyzed pituitary development in a series of FAT/DCHS mouse mutants (*Dchs1*, *Dchs2*, *Fat4*), which identified a range of infundibular and RP defects. Our data suggest a requirement for FAT and DCHS protocadherins in the infundibulum and mesenchyme surrounding the developing gland during morphogenesis, revealing that FAT/DCHS function is necessary for normal pituitary morphogenesis and their dysfunction can underlie developmental anomalies of the hypothalamic-pituitary axis.

Results

Molecular and *in silico* findings in patients with pituitary developmental defects

Combined with our description of expression of FAT/DCHS family members during pituitary development (27), the recent identification of links between DCHS abnormalities and pituitary developmental defects (8, 23) suggested an involvement of FAT/DCHS signaling in hypothalamic and/or pituitary development. To address this possibility, we studied 28 patients with congenital pituitary abnormalities of EPP and/or PSIS to whole exome sequencing, focusing on all four *FAT* genes, as well as *DCHS1* and *DCHS2*. Three heterozygous variants in DCHS2 and four in FAT2 were identified and their locations on the proteins summarized in a schematic (Figure 1A). The variants, their functional type, class (synonymous, non-synonymous, or frameshift), effect (missense, nonsense, silent), frequency in control database and the genes in which these variants were identified in

patients with EPP are presented in Table 1. The allele frequency of all variants in the cohort was 1.79%. Among all variants across these genes, only two variants in *DCHS2* and one variant in *FAT2* were classified as functionally 'high' and predicted to be deleterious using prediction tools (see Methods) (Table 1).

Clinical Data

The clinical and biochemical data of the six patients identified with *FAT2* and *DCHS2* variants are summarized in Table 2. Patient D190 was a 20.6-year-old male at the time of assessment, who was born full-term with cryptorchidism and micropenis. He was diagnosed with multiple anterior pituitary hormone deficiencies and learning difficulties and received full hormone replacement therapy. MRI showed EPP and a very small anterior pituitary for his age and sex (Figure 1B). The patient required testosterone treatment for micropenis and for pubertal induction and maintenance. Despite long-term follow-up, he never presented any increment in testicular volume. He was found to harbor a *DCHS2* stop codon c.C4027T (p.R1343*) variant (Table 1). This was also found in the atherosclerosis risk in communities study (ARIC) controls and is reported as a rare variant in the gnomAD database and likely deleterious based on the CADD prediction tool (Table 1).

Patient D041 was a 16.4-year-old male who was born full term. He developed growth hormone deficiency (GHD) and was treated with recombinant growth hormone (rGH) until the age of 16 years. His pituitary MRI revealed EPP and an anterior pituitary within the normal size range for his age and sex (Figure 1B). Molecular analysis revealed a synonymous *FAT2* variation F1497= (Table 1). This is reported as a very rare variant in the gnomAD database, although it is predicted to be likely benign based on CADD score (Table 1).

Patient D965 was a 13.9-year-old male at the time of assessment who was born at 34 weeks of gestation. He was diagnosed with GHD and MRI revealed an EPP (Table 2 and Figure 1B). He was still under rGH treatment during clinical assessment. Molecular analysis revealed a *FAT2* c.C10426T variant which creates a stop codon at p.R3476*. This variant was not found in any of the controls, it is reported as a very rare variant in the gnomAD database and it is likely deleterious according to the CADD prediction tool (Table 1). In addition, this patient was also found to harbor a variant in *DCHS2*: c.836_837delAAinsG (p.K279Sfs*10), that creates a frameshift resulting in premature termination of translation. This variant was not found in any of the controls and was absent from the gnomAD database (Table 1).

Patient D140 was a 20.7-year-old female who was born full-term. She was diagnosed with GHD following hypoglycemic seizures and received treatment with rGH (Table 2). Pituitary MRI revealed EPP and possible PSIS (Figure 1B, Table 2). She was found to harbor a *DCHS2* missense variant (p.T1328K) predicted to be damaging by all three prediction tools and has not been reported previously (Table 1).

Patient D831 was a 15.1-year-old male who was born pre-term at 31 weeks of gestation due to premature rupture of membranes. He was diagnosed with GH, TSH and partial ACTH deficiency as well as learning difficulties. He received rGH therapy until the age of 15 years and is now on replacement with Levothyroxine and steroids (Table 2). Pituitary MRI revealed EPP and possible PSIS (Figure 1B, Table 2). Molecular analysis revealed a *FAT2* p.R1250H missense variant absent from public databases, predicted as probably damaging by Polyphen, damaging by SIFT and likely deleterious by CADD. This was reported as very rare in the gnomAD database (Table 1).

Patient D205 was a 14.6-year-old male at the time of assessment. He was born at term with cryptorchidism and micropenis. He was diagnosed with GH and TSH deficiency and placed under replacement with rGH and Levothyroxine (Table 2). He also required testosterone treatment for micropenis and for pubertal induction and maintenance. MRI revealed EPP (Figure 1). He was found to harbor a *FAT2* missense variant (p.D2720H), not reported previously, and predicted to be probably damaging by Polyphen, damaging by SIFT and likely deleterious by CADD (Table 1).

DCHS2 and FAT2 are expressed during embryonic pituitary development

To explore whether the two genes contribute to pituitary development, we next examined expression of FAT2 and DCHS2 proteins in the developing human pituitary by immunostaining. At 17 post-conception weeks (pcw), DCHS2 expression was detected in mesenchymal cells around epithelial structures of the marginal zone as well as in diffuse mesenchymal cells within the anterior lobe (arrows, Figure 2A). FAT2 expression was also detected in mesenchymal cells, but also in the posterior lobe and at low levels in epithelial structures within the marginal zone (Figure 2B).

Specific cross-reactivity of the FAT2 antibody allowed us to carry out analysis in the mouse pituitary. At 14.5dpc, FAT2 was abundantly detected in the mesenchyme surrounding the developing gland, in invading mesenchymal tissue that will form the vasculature (4, 28), as well as in cells at the external layer of the rostral RP (arrows) contacting the mesenchyme, and in the infundibulum (arrowheads) (Figure 2C). Expression of *Fat2* and *Dchs2* in the mesenchyme surrounding the developing RP and infundibulum was confirmed by mRNA in situ hybridization (Supplementary Figure 1). At 18.5dpc just prior to birth, FAT2 expression

remained strong in mesenchyme surrounding the pituitary; there was expression in the posterior lobe and abundant signal detected throughout the vasculature of the anterior lobe (Figure 2D). By 10-weeks in the adult mouse pituitary, FAT2 expression persisted in the vasculature as confirmed by double immunofluorescence staining with Endomucin, marking endothelial cells of the blood vessels (arrows, Figure 2E).

Dchs2$^{-/-}$ mouse mutants have defects in hypothalamic-pituitary development

Considering the functional link suggested by the identification of PSIS patients with putatively pathogenic *DCHS2* variants, we next sought to confirm such implication using a *Dchs2* mutant mouse model. In order to confirm if DCHS2 has a function during hypothalamic-pituitary development, we analyzed *Dchs2*$^{-/-}$ null mutants. Gross inspection of the dissected mutant pituitary of neonates at P2 did not reveal any apparent morphological anomalies compared to controls (Supplementary Figure 2A, n=9). At 18.5dpc, a stage when morphogenesis of the HP axis has been fully achieved, and when PSIS-like anatomical phenotypes can be unambiguously detected, embryos exhibited mild anterior pituitary hypoplasia (3/6), accompanied by a significant reduction in the number of cycling cells as determined by antibody staining against Ki-67 (average 26.3% cycling cells in controls compared to 22.7% in mutants, P=0.0044 n=3, unpaired Student's t-test; Figure 3A). Analysis of cycling cells in the marginal zone surrounding the cleft and separately in the parenchyme revealed a reduction in both regions of mutants compared to controls (marginal zone P=0.0495, parenchyme P=0.007). We next sought to determine if anterior cell type commitment and differentiation occurred normally. Immunofluorescence staining using antibodies against commitment markers PIT1 (POU1F1), SF1 (NR5A1), TPIT (TBX19) in

179 *Dchs2*$^{-/-}$ and control *Dchs2*$^{+/+}$ pituitaries did not reveal differences between genotypes
180 (Figure 3B), confirmed by qRT-PCR (Supplementary Figure 2B, n=4). Similarly, no differences
181 were observed for the expression of differentiation markers ACTH, GH and TSH (n=3, Figure
182 3B) or for the expression of the stem cell marker *Sox2* (Supplementary Figure 2B). These
183 results are consistent with a role for DCHS2 in controlling morphogenesis rather than cell
184 fate specification within the AP.

185 Histological examination of frontal sections at 18.5dpc at anterior axial levels,
186 revealed dysmorphology of the median eminence and developing pituitary stalk in a
187 proportion of the mutants (4/6). Of note, the pituitary stalk in mouse is very short compared
188 to the developing human pituitary. Mutant embryos exhibited invaginations in the median
189 eminence and the epithelium of the infundibular recess (arrowheads Figure 3C, two mutant
190 embryos shown, axial levels as indicated in the cartoon). None of these anomalies were
191 observed in control littermates (n=8).

192

193 **_Fat4_$^{-/-}$ and _Dchs1_$^{-/-}$ mutants exhibit additional morphogenetic defects of the anterior**
194 **pituitary**

195 The observation of variability in penetrance of the *Dchs2*$^{-/-}$ null phenotypes suggested that
196 there might be some functional redundancy compensating for the loss of *Dchs2*. Indeed,
197 DCHS1 and DCHS2 act cooperatively during kidney development, acting with FAT4 as ligand-
198 receptor pair (24, 26). This led us to explore the possibility that other members of the
199 FAT/DCHS family might additionally contribute to pituitary development. We previously
200 detected strong expression of *Fat4* in the rostral tip of the developing murine pituitary
201 (which develops into the pars tuberalis), and strong expression of *Dchs1* in surrounding

mesenchyme (27). To characterize their expression during late pituitary development we carried out RNAscope mRNA *in situ* hybridization using specific probes against *Fat4* and *Dchs1* in sagittal sections through wild type pituitaries at 18.5dpc. *Fat4* expression was strong in the developing pars tuberalis, the developing posterior lobe and pituitary stalk, and transcripts were also detected in the surrounding mesenchyme and scattered cells of the developing anterior lobe. Low levels of *Dchs1* transcripts were detected throughout these tissues with the highest expression in the pituitary stalk (Figure 4A). To investigate if *Dchs1* expression increases in *Dchs2*$^{-/-}$ mutants, indicative of a compensatory mechanism, we carried out qRT-PCR on whole pituitary lysates comparing *Dchs2*$^{-/-}$ and *Dchs2*$^{+/-}$ control genotypes. Although not significant with the available samples, there appears to be an elevation of *Dchs1* mRNA levels in *Dchs2*$^{-/-}$ mutants (Supplementary Figure 2B, n=4 per genotype).

We hypothesized that loss of FAT4 or DCHS1 could also lead to pituitary defects. As neither *Fat4*$^{-/-}$ or *Dchs1*$^{-/-}$ mutants are viable past the early postnatal period, analysis was limited to embryonic stages and the perinatal period (P0-P2). As in *Dcsh2*$^{-/-}$ mutants, histological analysis of *Fat4*$^{-/-}$ mutants at 13.0dpc revealed abnormal invaginations in the epithelium of the infundibular recess in 7/10 embryos (arrowheads in Figure 4B). We also observed a severely abnormal invagination of the infundibulum lacking a central lumen, using mRNA *in situ* hybridization against *Fat3* to mark infundibular tissue (27) (1/10 embryos, Figure 4C). These infundibular anomalies were not observed in *Dchs1*$^{-/-}$ embryos (0/5 at 13.0dpc). The infundibular phenotypes shared between *Fat4*$^{-/-}$ and *Dchs2*$^{-/-}$ mutants suggest that FAT4 may be acting in concert with DCHS2, as receptor-ligand pair, during posterior pituitary development.

Upon gross examination at P0, both *Fat4*$^{-/-}$ and *Dchs1*$^{-/-}$ pituitaries exhibited shortening of the medio-lateral axis of the anterior pituitary compared to wild type littermates (Figure 4C), unlike *Dchs2*$^{-/-}$ mutants which did not display this phenotype (n=9, Supplementary Figure 2A). The size of the intermediate and posterior lobes was comparable to wild type controls (n=8 for *Fat4*$^{-/-}$, n=10 for *Dchs1*$^{-/-}$). Analysis of proliferation by Ki-67 immunostaining did not reveal differences in the number of cycling cells between genotypes (Supplementary Figure 3, n=3 per genotype). Immunofluorescence staining of lineage commitment and differentiation markers of the anterior pituitary (PIT1, SF1, TPIT, GH, TSH, ACTH) identified normal distribution of committed and differentiated cell types in *Fat4*$^{-/-}$ pituitaries compared to controls (n=3, Figure 4D). No differences were observed between *Fat4*$^{-/-}$ and *Dchs1*$^{-/-}$ genotypes (not shown).

Discussion

Screening 28 patients with EPP and/or PSIS, we have identified seven variants in *FAT2* and *DCHS2* in six patients. Five of these variants were predicted to be damaging by *in silico* analysis. Indeed, the existence of familial cases with mutations and/or single nucleotide variants in genes involved in the developmental process such as in *HESX1*, *LHX4*, *PROP1*, *OTX2*, *SOX3*, *PROKR2* and *GPR161* have suggested a Mendelian form of inheritance (6, 7, 29). Recently, Zwaveling-Soonawala et al, also identified *DCHS1* as one of the candidate genes for sporadic PSIS in two young patients: a nine year old female who presented with absent stalk and anterior pituitary, EPP and hormonal deficiencies and a 2.5 year old male with small stalk and anterior pituitary, EPP and hormonal deficiencies (8). Although no functional studies were performed, both these patients had variants in other genes that

were also predicted to be damaging, such as in *GLI2* which has been reported to be involved in holoprosencephaly and abnormal pituitary development (30) and in *BMP4*, which has a crucial role during embryonic pituitary development (31) indicating that variants in one or more genes other than *FAT2* and *DCHS2* may be required for an apparent phenotype.

In our screen, all patients with *FAT2* or *DCHS2* variants had GHD and three of them had combined hormone deficiency. Two of these patients had a more severe phenotype with complete deficiency of the adenohypophysis and a pituitary height smaller than expected for their age and sex.

Considering that in all *Dchs* and *Fat* mouse mutants analyzed, anterior cell type commitment and differentiation occurred normally, the hormonal deficiencies identified in our patients could be due to the lack of trophic signals of the hypothalamic releasing factors rather than defects in the differentiation of the anterior endocrine cells. In the patients, we were not able to identify a specific phenotype-genotype correlation, which indicates that these variants can be confounding factors, or causative where other factors also contribute to the severity of symptoms.

Expression analysis of both mouse and human tissue revealed that in development, FAT/DCHS protocadherins are expressed in the mesenchyme surrounding the pituitary. The infundibulum and posterior pituitary gland receive a rich blood supply from the superior hypophyseal artery, infundibular artery and inferior hypophyseal artery (32), all of mesenchymal origin (28, 33). Disruption of the pituitary vascular network can result in abnormal tissue morphology and poor function (28, 33). We postulate that mutations in *FAT2* and *DCHS2* may affect the development of the posterior lobe and its connection to the hypothalamus, through affecting the surrounding mesenchymal contribution. By analyzing

developing *Dchs2*$^{-/-}$ mouse mutant pituitaries, we have identified a partially penetrant pituitary stalk defect as well as anterior pituitary hypoplasia. Like *Fat2*$^{-/-}$ mice however, these have previously been described as normal, healthy and viable, possibly due to the redundant roles with other FAT and DCHS family members (26, 34). Consistent with this stalk phenotype, we also identified abnormal infundibular development in *Fat4*$^{-/-}$ mutants, previously shown to exhibit poor cerebral neuronal migration (14, 35). As such, the ventral migration of axons of hypothalamic neurons located in the paired supraoptic and paraventricular nuclei, which terminate in the posterior pituitary (4), might also be affected by loss of FAT/DCHS protocadherins, resulting in abnormal evagination of this tissue and PSIS.

Interestingly, analysis of *Fat4*$^{-/-}$ as well as *Dchs1*$^{-/-}$ single mutants revealed an additional pituitary defect, shortening of the medio-lateral axis of the anterior lobe. As this is consistent between the two genotypes, we conclude that FAT4 and DCHS1, expressed in the developing RP, infundibulum and surrounding mesenchyme (27), are likely acting as receptor-ligand pair in the morphogenesis of the anterior lobe, and we hypothesize that expression of both proteins in the surrounding mesenchyme is critical for this process (27). FAT4/DCHS1 may be involved in cell movements during development, which is consistent with their known role in planar cell polarity (10, 11, 25), often an important pathway during dynamic rearrangement and migration of cells. In the anterior pituitary they are unlikely to act upstream of YAP for this purpose, as previous work deregulating YAP levels during development did not result in medio-lateral morphogenesis defects (36).

Taken together, our studies have revealed a requirement for the concerted action of FAT/DCHS protocadherins for normal pituitary development and support the pathogenicity

294 of *FAT2* and *DCHS2* variants in patients with ectopic PSIS in addition to other genes reported
295 (8). As PSIS may present with isolated or multiple hormonal deficiencies, then neonatal
296 hypoglycemia, micropenis and/or cryptorchidism with or without growth deficit should
297 prompt early screening with hormonal and imaging investigations for early detection and
298 treatment. Furthermore, genetic screening for identification of a specific mutation in the
299 genes involved in PSIS development is a prerequisite for genetic counseling and appropriate
300 long-term follow-up, which is imperative as there is a strong possibility of development of
301 other hormonal insufficiencies.

Methods

Whole exome sequencing of patients with ectopic posterior pituitary

The data from 28 unrelated patients diagnosed with non-syndromic EPP were reviewed and DNA was extracted from peripheral blood mononuclear cells. Whole exome sequencing and variant calling were performed for *FAT1*, *FAT2*, *FAT3*, *FAT4*, *DCHS1* and *DCHS2*. DNA samples from 156 in-house parents of osteosarcoma patients and 8,554 from Atherosclerosis Risk in Communities Study (ARIC) database were used as controls.

Analysis of the identified variants

The variants that were identified in controls were filtered and analysis was focused on the variants with functional type “high” and “moderate”. Allele frequencies identified in patients with EPP were compared to allele frequency published on reference database The Genome Aggregation Database (gnomAD) spans 125,748 exome sequences and 15,708 whole-genome sequences from unrelated individuals and publicly available online (https://gnomad.broadinstitute.org). The possible functional impact of an amino acid substitution was predicted by three different in silico prediction tools: (1) the PolyPhen (Polymorphism Phenotyping) program (http://genetics.bwh.harvard.edu/pph2) which calculates the position-specific independent counts (PSIC) score that represents the probability that a substitution be damaging; values nearer to 1 are more confidently predicted to be deleterious, (2) for missense variants, the Sorting Intolerant From Tolerant (SIFT) program [http://sift.jcvi.org] calculates normalized probabilities for all possible substitutions from the alignment. Positions with normalized probabilities less than 0.05 are predicted to be deleterious; those greater than or equal to 0.05 are predicted tolerated. (3)

The Combined Annotation Dependent Depletion score (CADD, v1.3, https://www.ncbi.nlm.nih.gov/pubmed/30371827) which combines deleteriousness predictions from multiple algorithms into a single phred-like score for all possible single nucleotide variants in the genome (i.e. a CADD score >10 is predicted to be amongst the top 10% most deleterious single nucleotide variants in the genome, CADD score >20 is amongst the top 1%, CADD score >30 is amongst the top 0.1%, etc). For convenience we classified the variants with a CADD score >20 as 'likely deleterious' and below 20 as 'likely benign'.

Animals

Dchs2$^{-/-}$, *Fat4*$^{fl/fl}$ and *Dchs1*$^{-/-}$ animals were previously described (24-26). For the generation of *Fat4*$^{-/-}$ animals, *Fat4*$^{fl/fl}$ mice were crossed with the *Actb*$^{Cre/+}$ strain for ubiquitous deletion (37) and offspring were intercrossed. For embryo collection, the morning of vaginal plug was considered 0.5dpc. Embryos or postnatal pituitaries were dissected, fixed in 10% NBF overnight with agitation, then dehydrated through an ascending ethanol series. Tissues were processed for paraffin embedding and sectioned to 4µm for RNAscope mRNA *in situ* hybridization, or 7µm for hematoxylin and eosin staining and immunofluorescence.

Hematoxylin and eosin staining

Slides were dewaxed in Histoclear (National Diagnostics) and rehydrated through a descending ethanol series in dH_2O. Sections were stained with Harris' hematoxylin and eosin following standard protocols. Slides were dehydrated and dried, then coverslips mounted with VectaMount (Vector Ltd).

RNAscope mRNA *in situ* hybridization

Sections were processed and stained as described previously (27). Briefly, slides were heated to 60°C, dewaxed in xylene and washed in 100% ethanol and processed following the RNAscope 2.5HD Reagent Kit-RED assay kit (Advanced Cell Diagnostics) with specific probes (*Fat4*, *Dchs1, Fat3*). Following detection, slides were weakly counterstained with hematoxylin and coverslips mounted with VectaMount (Vector Ltd).

Immunofluorescence (IMF)

Slides were deparaffinized in Histoclear, rehydrated through a descending ethanol series, followed by antigen retrieval in pH6.0 citrate buffer in a NXGEN Decloaking Chamber (Menari Diagnostics) at 110°C for 3min. Slides were washed in PBST (PBS with 0.1% Triton-X), blocked in Blocking Buffer (0.15% glycine, 2mg/ml BSA, 0.1% Triton-X in PBS) with 10% sheep serum for 1h at room temperature, then incubated overnight in primary antibody in Blocking Buffer with 1% sheep serum at 4°C. Primary antibodies used were against: DCHS2 (1:500, Atlas HPA064159), FAT2 (1:1000, Santa Cruz sc59985), Ki-67 (1:300, Abcam ab16667), SOX2 (1:300, Abcam ab97959), PIT1 (1:1000, gift from Prof. S. Rhodes, University of North Florida, USA), TPIT (1:300, gift from Prof. J. Drouin, University of Montreal, Canada), SF1 (1:300, Life Technologies N1665), ACTH (1:300, Fitzgerald 10C-CR1096M1), GH (1:1000, NHPP AFP5641801), TSH (1:1000 NHPP AFP-1274789). The Vector ImmPRESS kit was used for antibodies against SF1 according to the manufacturer's instructions. The PerkinElmer TSA kit was used for antibodies against DCHS2 and FAT2, as previously described (36). After primary antibody incubation, slides were washed in PBST then incubated with appropriate secondary antibodies (biotinylated goat anti-rabbit (1:300, Abcam ab6720), biotinylated goat anti-mouse (1:300 Abcam ab6788)), and incubated with fluorophore-conjugated Streptavidin (1:500, Life Technologies S11223) for 1h at room

temperature. Quenching of endogenous autofluorescence was carried out by treatment with Sudan Black B following immunofluorescence against TPIT and SF1. Nuclei were counterstained with Hoechst (1:10000, Life Technologies H3570). Coverslips were mounted with VectaMount (Vector Laboratories, H1000).

Imaging

Wholemount images were taken with a MZ10 F Stereomicroscope (Leica Microsystems), using a DFC3000 G camera (Leica Microsystems). For bright field images, stained slides were scanned with Nanozoomer-XR Digital slide scanner (Hamamatsu) and images processed using Nanozoomer Digital Pathology View. Immunofluorescent staining was imaged with a TCS SP5 confocal microscope (Leica Microsystems) and images processed using Fiji (38).

Proliferation analysis

The number of Ki-67 positive cells and total nuclei stained with Hoechst, were counted manually using Fiji (at least 5000 nuclei counted over 5-7 sections per biological sample) for control and mutant pituitaries, n=3 per genotype. Nuclei along the marginal zone epithelium were recorded separately to those within the anterior pituitary parenchyme.

Quantitative RT-PCR

Whole pituitaries were dissected from 10 week old *Dchs2*$^{+/-}$ (control) and *Dchs2*$^{-/-}$ (mutant) mice and placed in RNAlater-ice (Thermo Fisher, AM7030). They were flash frozen in liquid nitrogen and stored at -80°C. mRNA was extracted using Monarch Total RNA Miniprep kit (New England Biolabs, T2010S), translated using QuantiTect Reverse Transcription kit (Qiagen, 205311) then qRT-PCR was performed using QuantiNova SYBR Green RT-PCR kit (Qiagen, 208152) on a Roche Lightcycler 480. Data were analyzed using delta delta CT

method normalized to housekeeping gene expression, n=4 pituitaries per genotype. Primers used: *Pou1f1* (*Pit1)* fw CACGGCTCAGAATTCAGTCA, rv TCCAGAGCATCCTTAGCAGC; *Tbx19 (Tpit)* fw TGTCTCGCCTGCTTAACGTG, rv GACAGGGAACATCCGTCTGC; *Nr5a1 (Sf1)* fw AGCTGCAAGGGCTTCTTCAA, rv CATTCGATCAGCACGCACAG; *Sox2* fw GAGGGCTGGACTGCGAACT, rv TTTGCACCCCTCCCAATTC; *Dchs1* fw TCCACGTTCATCCACTCAGC, rv GGGGACTGTTCTCACGAAGG; *Hprt* (housekeeping) fw GTTGGGCTTACCTCACTGCT, rv TCATCGCTAATCACGACGCT; *Actb* (housekeeping) fw TTCTTTGCAGCTCCTTCGTT, rv ATGGAGGGGAATACAGCCC.

Statistics

Data were analyzed using two-tailed unpaired Student's t-tests using the Holm-Sidak method to correct for multiple analysis, where $P<0.05$ was taken to be statistically significant.

Study Approval

All participants, or their legal guardian, provided written and informed consent. The present studies in humans were reviewed and approved by the Irmandade da Santa Casa de Misericórdia de São Paulo review board (project number 34003914.0.0000.5479), located at Marquês de Itu Street, 381, São Paulo, Brazil. Animal husbandry was carried out under compliance of the Animals (Scientific Procedures) Act 1986, relevant Home Office License (P5F0A1579) and KCL Ethical Review approval.

AUTHOR CONTRIBUTIONS

Designing research studies: FH, CAS, CLA; conducting experiments: EJL, PX, AS, TSS, FRF, DS, ALP; acquiring data: EJL, PX, TSS, CK, CAL, AS, JLM, NP, JL, CLA; analyzing data: EJL, PX, AS, FRF; providing reagents: TH, PF-W, FH, CAS; writing the manuscript: PX, EJL, CLA; editing the manuscript: PF-W, FH, JLM, CAS.

ACKNOWLEDGEMENTS

We thank the patients and their families for participating in the described studies. This study was supported by grants MR/L016729/1 from the MRC (CLA), a Lister Institute Research Prize Fellowship to CLA, RG130699 from The Royal Society (CLA), the Deutsche Forschungsgemeinschaft (DFG) within the 314061271 - TRR 205 (CLA), the AFM-Téléthon (Association Française contre les myopathies) grant 20861 (FH), grant BB/M022544/1 from the BBSRC (PF-W). This study was in part funded by the intramural research program of the *Eunice Kennedy Shriver* National Institute of Child Health of Human Development (NICHD), Bethesda, MD20892, USA. We are grateful to Prof. Jacques Drouin and Prof. Simon Rhodes for TPIT and PIT antibodies respectively, and the National Hormone and Peptide Program (Harbor-University of California, Los Angeles Medical Center) for providing some of the hormone antibodies used in this study. We thank Prof. Kenneth Irvine for continued advice and sharing reagents and Prof. Helen McNeill for providing the *Fat4* mouse mutant.

References

1. Bar C, et al. Pituitary Stalk Interruption Syndrome from Infancy to Adulthood: Clinical, Hormonal, and Radiological Assessment According to the Initial Presentation. *PloS one.* 2015;10(11):e0142354.

2. Voutetakis A, Sertedaki A, Dacou-Voutetakis C. Pituitary stalk interruption syndrome: cause, clinical manifestations, diagnosis, and management. *Current opinion in pediatrics.* 2016;28(4):545-550.

3. Fujisawa I, et al. Transection of the pituitary stalk: development of an ectopic posterior lobe assessed with MR imaging. *Radiology.* 1987;165(2):487-489.

4. Cheung LY, Davis SW, Brinkmeier ML, Camper SA, Perez-Millan MI. Regulation of pituitary stem cells by epithelial to mesenchymal transition events and signaling pathways. *Mol Cell Endocrinol.* 2017;445:14-26.

5. Tatsi C, et al. Pituitary stalk interruption syndrome and isolated pituitary hypoplasia may be caused by mutations in holoprosencephaly-related genes. *J Clin Endocrinol Metab.* 2013;98(4):E779-784.

6. Reynaud R, et al. PROKR2 variants in multiple hypopituitarism with pituitary stalk interruption. *J Clin Endocrinol Metab.* 2012;97(6):E1068-1073.

7. Reynaud R, et al. Pituitary stalk interruption syndrome in 83 patients: novel HESX1 mutation and severe hormonal prognosis in malformative forms. *European journal of endocrinology.* 2011;164(4):457-465.

8. Zwaveling-Soonawala N, et al. Clues for Polygenic Inheritance of Pituitary Stalk Interruption Syndrome From Exome Sequencing in 20 Patients. *J Clin Endocrinol Metab.* 2018;103(2):415-428.

9. Tanoue T, Takeichi M. New insights into Fat cadherins. *Journal of cell science.* 2005;118(Pt 11):2347-2353.

10. Mao Y, et al. Dchs1-Fat4 regulation of polarized cell behaviours during skeletal morphogenesis. *Nature communications.* 2016;7:11469.

11. Zakaria S, et al. Regulation of neuronal migration by Dchs1-Fat4 planar cell polarity. *Current biology : CB.* 2014;24(14):1620-1627.

12. Ragni CV, et al. Amotl1 mediates sequestration of the Hippo effector Yap1 downstream of Fat4 to restrict heart growth. *Nature communications.* 2017;8:14582.

13. Crespo-Enriquez I, et al. Dchs1-Fat4 regulation of osteogenic differentiation in mouse. *Development (Cambridge, England).* 2019;146(14).

14. Cappello S, et al. Mutations in genes encoding the cadherin receptor-ligand pair DCHS1 and FAT4 disrupt cerebral cortical development. *Nature genetics.* 2013;45(11):1300-1308.

15. Blair S, McNeill H. Big roles for Fat cadherins. *Current opinion in cell biology.* 2018;51:73-80.

16. Rock R, Schrauth S, Gessler M. Expression of mouse dchs1, fjx1, and fat-j suggests conservation of the planar cell polarity pathway identified in Drosophila. *Developmental*

dynamics : an official publication of the American Association of Anatomists. 2005;234(3):747-755.

17. Ivanovski I, et al. Van Maldergem syndrome and Hennekam syndrome: Further delineation of allelic phenotypes. *American journal of medical genetics Part A.* 2018;176(5):1166-1174.

18. Alders M, et al. Hennekam syndrome can be caused by FAT4 mutations and be allelic to Van Maldergem syndrome. *Human genetics.* 2014.

19. Mansour S, et al. Van Maldergem syndrome: further characterisation and evidence for neuronal migration abnormalities and autosomal recessive inheritance. *European journal of human genetics : EJHG.* 2012;20(10):1024-1031.

20. Zampino G, et al. Cerebro-facio-articular syndrome of Van Maldergem: confirmation of a new MR/MCA syndrome. *Clinical genetics.* 1994;45(3):140-144.

21. van Maldergem L, Wetzburger C, Verloes A, Fourneau C, Gillerot Y. Mental retardation with blepharo-naso-facial abnormalities and hand malformations: a new syndrome? *Clinical genetics.* 1992;41(1):22-24.

22. Hennekam RC, et al. Autosomal recessive intestinal lymphangiectasia and lymphedema, with facial anomalies and mental retardation. *American journal of medical genetics.* 1989;34(4):593-600.

23. Sotos J, et al. A patient with van Maldergem syndrome with endocrine abnormalities, hypogonadotropic hypogonadism, and breast aplasia/hypoplasia. *International journal of pediatric endocrinology.* 2017;2017:12.

24. Mao Y, et al. Characterization of a Dchs1 mutant mouse reveals requirements for Dchs1-Fat4 signaling during mammalian development. *Development (Cambridge, England).* 2011;138(5):947-957.

25. Saburi S, et al. Loss of Fat4 disrupts PCP signaling and oriented cell division and leads to cystic kidney disease. *Nature genetics.* 2008;40(8):1010-1015.

26. Bagherie-Lachidan M, et al. Stromal Fat4 acts non-autonomously with Dachsous1/2 to restrict the nephron progenitor pool. *Development (Cambridge, England).* 2015.

27. Lodge EJ, Russell JP, Patist AL, Francis-West P, Andoniadou CL. Expression Analysis of the Hippo Cascade Indicates a Role in Pituitary Stem Cell Development. *Frontiers in physiology.* 2016;7:114.

28. Davis SW, et al. beta-catenin is required in the neural crest and mesencephalon for pituitary gland organogenesis. *BMC developmental biology.* 2016;16(1):16.

29. Fang Q, et al. Genetics of Combined Pituitary Hormone Deficiency: Roadmap into the Genome Era. *Endocrine reviews.* 2016;37(6):636-675.

30. Arnhold IJ, Franca MM, Carvalho LR, Mendonca BB, Jorge AA. Role of GLI2 in hypopituitarism phenotype. *J Mol Endocrinol.* 2015;54(3):R141-150.

31. Ericson J, Norlin S, Jessell TM, Edlund T. Integrated FGF and BMP signaling controls the progression of progenitor cell differentiation and the emergence of pattern in the embryonic anterior pituitary. *Development (Cambridge, England).* 1998;125(6):1005-1015.

32. Ciofi P, et al. Brain-endocrine interactions: a microvascular route in the mediobasal hypothalamus. *Endocrinology.* 2009;150(12):5509-5519.

33. Scully KM, et al. Epithelial cell integrin β1 is required for developmental angiogenesis in the pituitary gland. *Proceedings of the National Academy of Sciences.* 2016;113(47):13408-13413.

34. Barlow JL, et al. A p53-dependent mechanism underlies macrocytic anemia in a mouse model of human 5q- syndrome. *Nature medicine.* 2010;16(1):59-66.

35. Zakaria S, et al. Regulation of neuronal migration by dchs1-fat4 planar cell polarity. *Current biology : CB.* 2014;24(14):1620-1627.

36. Lodge EJ, et al. Homeostatic and tumourigenic activity of SOX2+ pituitary stem cells is controlled by the LATS/YAP/TAZ cascade. *eLife.* 2019;8.

37. Lewandoski M, Meyers EN, Martin GR. Analysis of Fgf8 gene function in vertebrate development. *Cold Spring Harb Symp Quant Biol.* 1997;62:159-168.

38. Schindelin J, et al. Fiji: an open-source platform for biological-image analysis. *Nature methods.* 2012;9(7):676-682.

Figure 1. Variants in FAT2 and DCHS2 in patients with PSIS. (**A**) Representative schematic of the FAT2 and DCHS2 proteins indicating the locations of identified mutations. Variants in red are predicted likely deleterious by CADD score (>20). No CADD score data available for DCHS2 p.K279Sfs*10. (**B**) Sagittal T1 pituitary MRIs of the six patients with *FAT2*/*DCHS2* variants and normal MRI for comparison, bottom left. For each patient, the normal posterior pituitary bright spot is not seen in the pituitary fossa, rather, an ectopic small region of high T1 signal at the top of the infundibulum or higher (red arrows). PS: pituitary stalk, AP: anterior pituitary, PP: posterior pituitary (normal intrasellar).

Figure 1

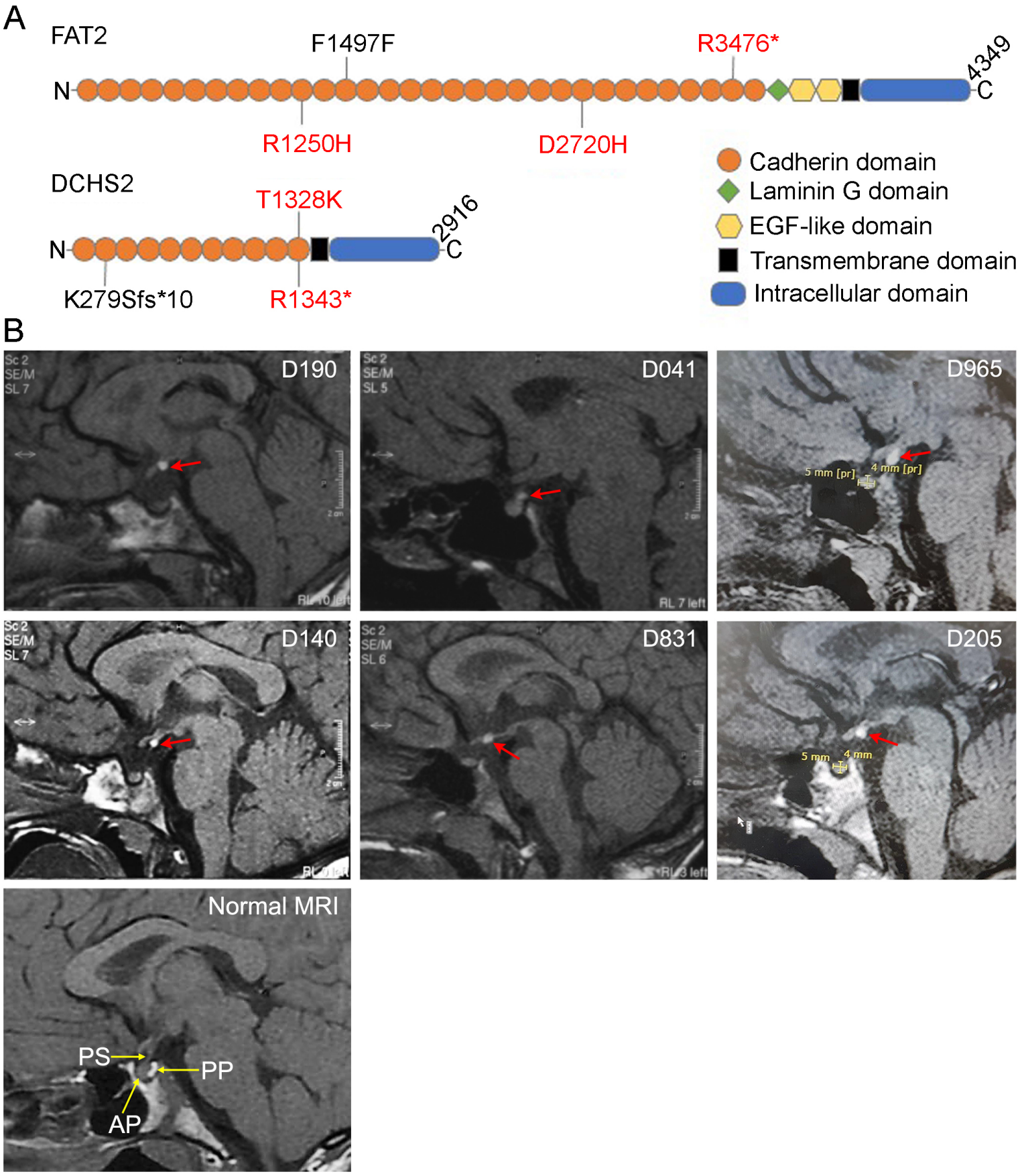
A
FAT2
F1497F
R3476*
N
4349
C
R1250H
D2720H
DCHS2
T1328K
2916
N
C
K279Sfs*10
R1343*
Cadherin domain
Laminin G domain
EGF-like domain
Transmembrane domain
Intracellular domain
B
D190
D041
D965
5 mm [pr]
4 mm [pr]
D140
D831
D205
5 mm
4 mm
Normal MRI
PS
PP
AP

Figure 2. **DCHS2 and FAT2 expression in the developing pituitary.** (**A,B**) Immunofluorescence staining on 17 post-conception week (pcw) human fetal pituitary sections, using specific antibodies against DCHS2 (A) and FAT2 (B), n=2. DCHS2 is expressed in mesenchymal tissues surrounding epithelial structures in the marginal zone, between the posterior and anterior pituitary and within the anterior lobe (arrows). FAT2 localizes in mesenchymal tissues within the anterior lobe, is expressed throughout the posterior lobe and diffuse staining is observed in epithelial structures in the marginal zone. Images in (i) and (ii) are magnified boxed regions in (A) and (B). (**C,D**) Immunofluorescence staining using antibodies against FAT2 on the developing mouse pituitary at 14.5 days post coitum (dpc) (C) and 18.5dpc (D), n=3. At 14.5dpc FAT2 localizes in mesenchymal tissue Rathke's pouch (RP), in cells of (RP) making contact with the mesenchyme (arrows) and in cells of the infundibulum (arrowheads) (C). At 18.5dpc, FAT2 expression persists in the mesenchyme surrounding the gland, throughout the posterior lobe and in vasculature throughout the anterior lobe (D). (**E**) In the wild type adult pituitary at 10 weeks, FAT2 (green) is expressed strongly by cells of the vasculature, as seen by double-immunofluorescence staining with Endomucin (red) marking endothelial cells (E), n=3. PL: posterior lobe, AL: anterior lobe, IL: intermediate lobe, MZ: marginal zone, Inf: infundibulum, RP: Rathke's pouch, M: mesenchyme, Sph: sphenoid bone, BV: blood vessels. Scale bars: 200μm in (A-C), 100μm in (E).

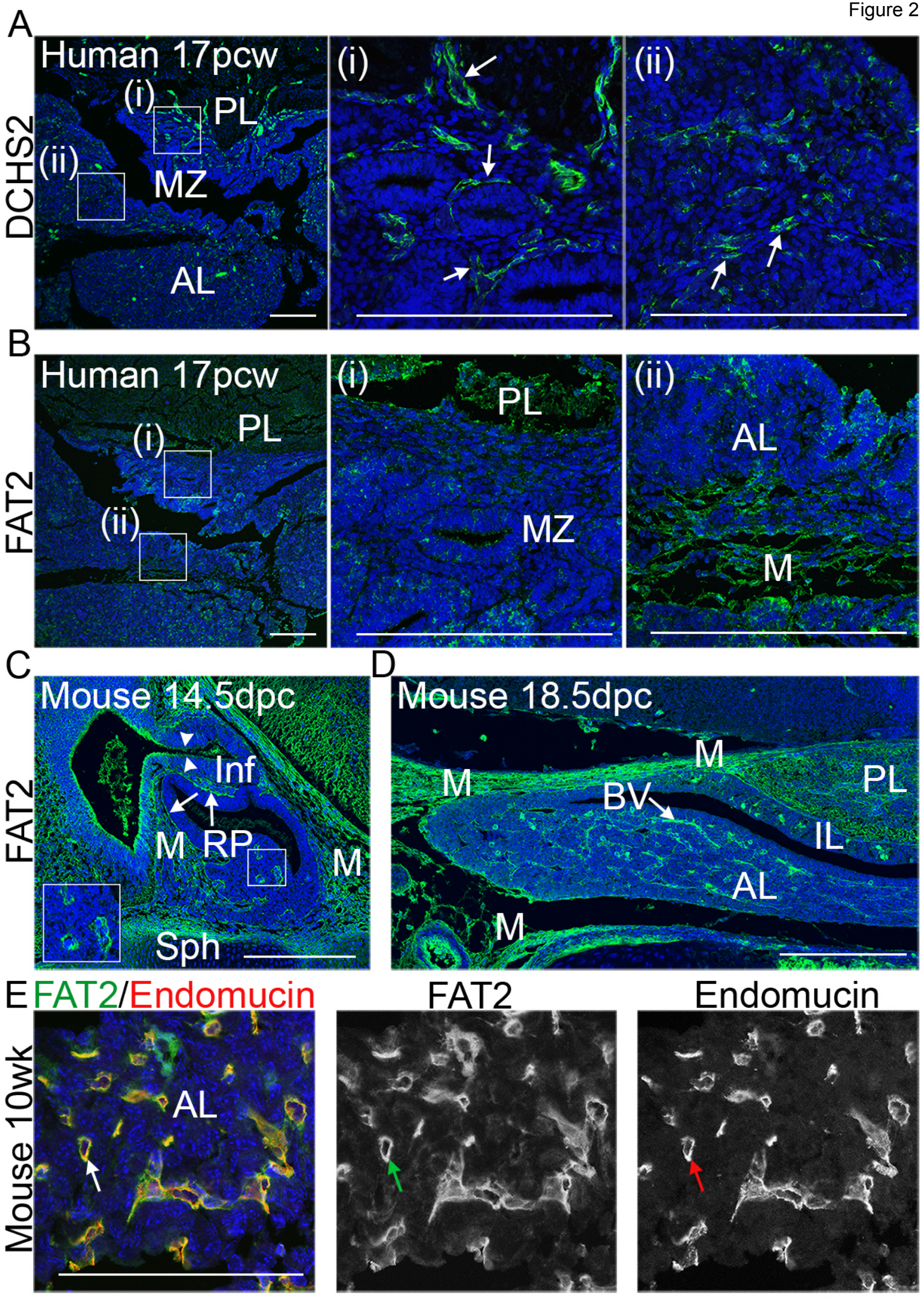
A
Human 17pcw
(i)
PL
(ii)
MZ
AL
DCHS2
(i)
(ii)
B
Human 17pcw
(i)
PL
(ii)
FAT2
(i)
PL
MZ
(ii)
AL
M
C
Mouse 14.5dpc
Inf
M
RP
M
Sph
FAT2
D
Mouse 18.5dpc
M
M
BV
PL
IL
AL
M
E
FAT2/Endomucin
AL
Mouse 10wk
FAT2
Endomucin

Figure 3. DCHS2 is required for normal murine pituitary development. (**A**) Immunofluorescence staining using antibodies against Ki-67 to detect cycling cells, on frontal sections of pituitaries from *Dchs2*$^{-/-}$ mutants and wild type littermate controls at 18.5dpc. Graph depicting quantification of cycling cells of the anterior pituitary of wild type controls and *Dchs2*$^{-/-}$ mutants, showing reduced proliferation in mutants in the marginal zone (MZ) surrounding the cleft *P*=0.0495, parenchyme (Par) *P*=0.007 and total throughout the anterior lobe *P*=0.0044, unpaired Student's t-test (n=3 per genotype, multiple sections counted). Values of Ki-67 positive cells are expressed as a percentage of the total nuclei in the anterior lobe. Average values are indicated. (**B**) Immunofluorescence staining on *Dchs2*$^{-/-}$ pituitaries and littermate controls at 18.5dpc (n=3) using antibodies against lineage-committed progenitor markers PIT1 (thyrotrophs, somatotrophs, lactotrophs), SF1 (gonadotrophs) and TPIT (corticotrophs, melanotrophs) and hormones TSH, GH and ACTH expressed in differentiated thyrotrophs, somatotrophs and corticotrophs, respectively. Staining is comparable for all markers between genotypes. (**C**) Hematoxylin and eosin staining on frontal sections of *Dchs2*$^{-/-}$ mutants and control at 18.5dpc at axial levels as indicated in the cartoon (n=6). Abnormal invaginations are seen in the median eminence (arrowheads) as wells as lobulated protrusions (arrow). PL: posterior lobe, IL: intermediate lobe, AL: anterior lobe, Hyp: hypothalamus, M: mesenchyme, Sph: sphenoid bone. Scale bars: 200μm in (A) and (B), 250μm in (C).

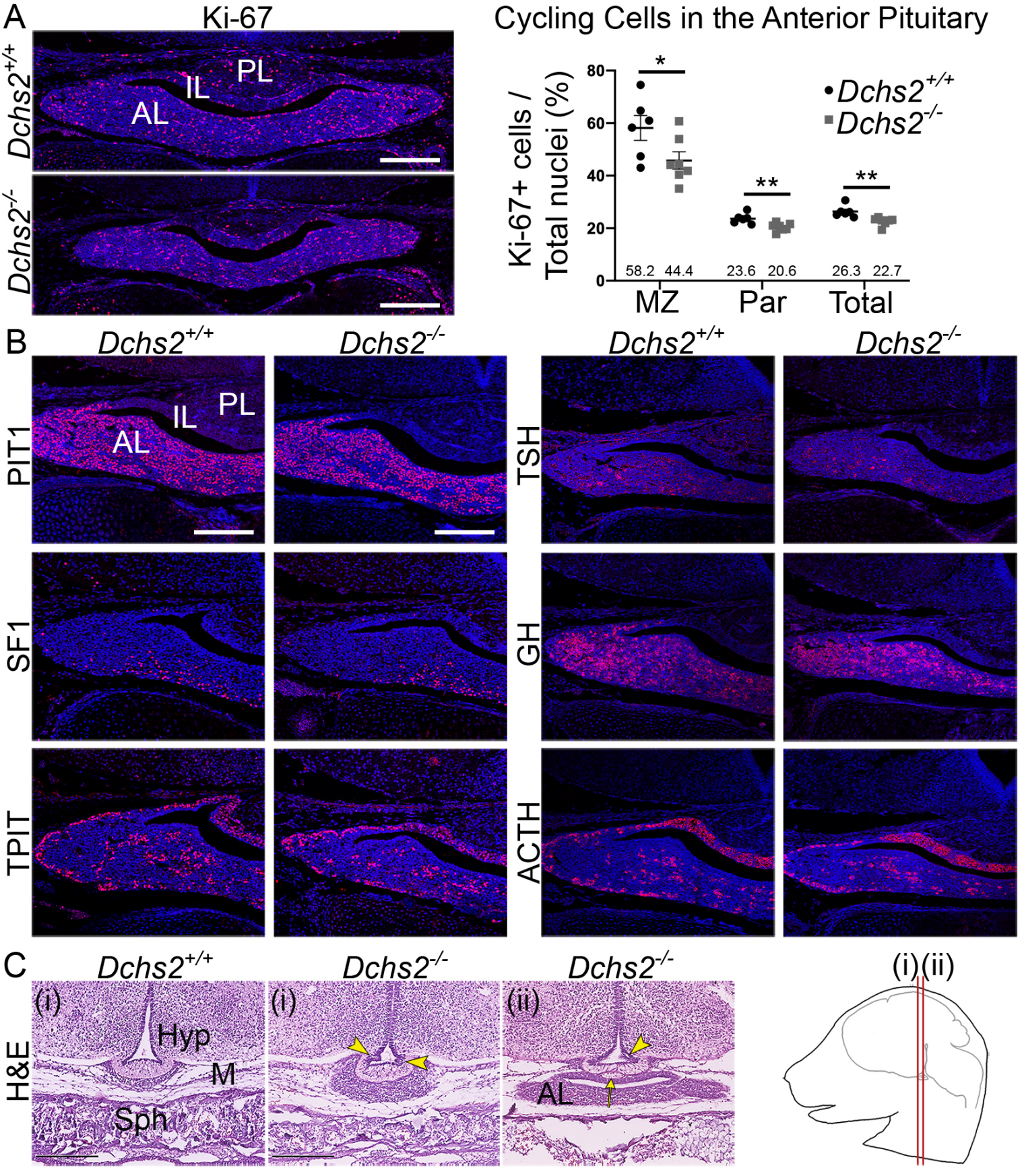
A
Ki-67
Dchs2+/+
Dchs2-/-
PL
IL
AL
Cycling Cells in the Anterior Pituitary
Ki-67+ cells / Total nuclei (%)
Dchs2+/+
Dchs2-/-
*
**
**
58.2 44.4
23.6 20.6
26.3 22.7
MZ
Par
Total
B
Dchs2+/+
Dchs2-/-
PIT1
TSH
SF1
GH
TPIT
ACTH
C
H&E
(i)
(ii)
Hyp
M
Sph
AL

Figure 4. FAT4 and DCHS1 are required for normal murine pituitary development. (**A**) RNAscope mRNA *in situ* hybridization on sagittal sections through wild type murine pituitaries at 18.5dpc using probes against *Fat4* and *Dchs1* (n=3). Abundant *Fat4* transcripts are detected in the pars tuberalis, the infundibulum, developing pituitary stalk and mesenchyme surrounding definitive Rathke's pouch. Some transcripts are also detected in RP. Expression of *Dchs1* is detected at low levels throughout these tissues. (**B**) Hematoxylin and eosin staining of sagittal sections through *Dchs1*$^{-/-}$ (n=5), *Fat4*$^{-/-}$ (n=10) and control pituitaries (n=15) at 13.0dpc showing invaginations in the infundibulum of *Fat4*$^{-/-}$ mutants (arrowheads), not observed in control or *Dchs1*$^{-/-}$ embryos. RNAscope mRNA *in situ* hybridization on sagittal sections through control wild type and *Fat4*$^{-/-}$ pituitaries at 13.5dpc using specific probes against *Fat3* marking the ventral diencephalon and infundibulum, which is abnormal in mutants (arrowheads). (**C**) Wholemount images taken at dorsal (top panels) and frontal views (bottom panel) of control, *Dchs1*$^{-/-}$ (n=10) and *Fat4*$^{-/-}$ (n=8) pituitaries at P0. Both *Dchs1*$^{-/-}$ and *Fat4*$^{-/-}$ mutants have a shortened medio-lateral axis affecting the anterior lobe compared to control. (**D**) Immunofluorescence staining on *Fat4*$^{-/-}$ pituitaries and littermate controls at 18.5dpc using antibodies against lineage-committed progenitor markers PIT1, TPIT and SF1 and hormones TSH, GH and ACTH (n=3). Staining is comparable for all markers between genotypes. Inf: infundibulum, PS: pituitary stalk, PT: pars tuberalis, RP: Rathke's pouch, M: mesenchyme, VD: ventral diencephalon, PL: posterior lobe, IL: intermediate lobe, AL: anterior lobe. Scale bars: 250μm in (A) and (B), 100μm in (D).

Figure 4

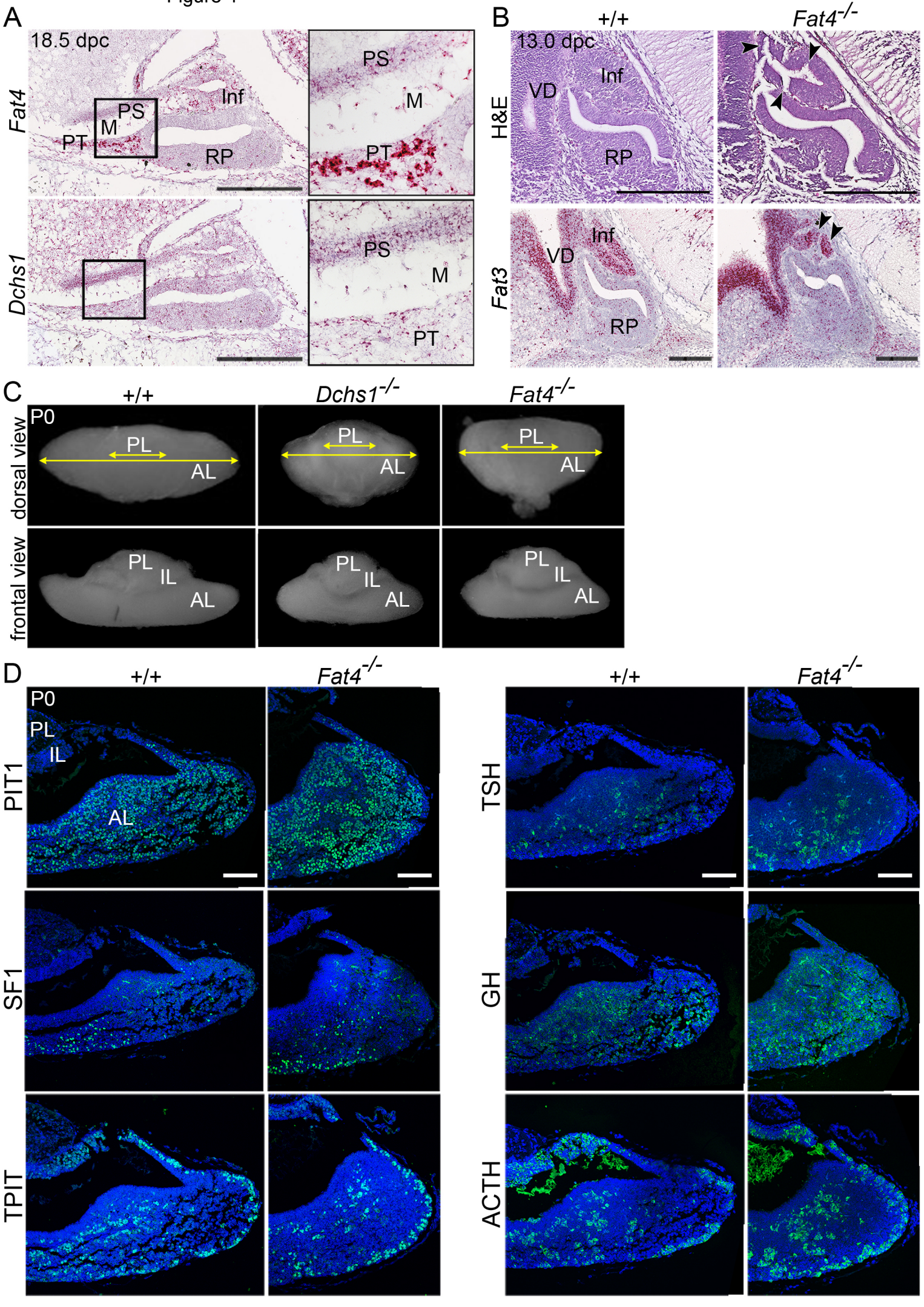
A
18.5 dpc
Fat4
Dchs1
Inf
PS
M
PT
RP
B
+/+
Fat4-/-
13.0 dpc
H&E
Fat3
VD
Inf
RP
C
+/+
Dchs1-/-
Fat4-/-
P0
dorsal view
frontal view
PL
AL
IL
D
+/+
Fat4-/-
PIT1
SF1
TPIT
TSH
GH
ACTH

TABLES

Table 1. Mutations/variations of *FAT*/*DCHS* identified in patients with EPP

Patient Code	Gene	Functional Type	Func. refGene	SNP Effect	Functional Class	Codon Change	Amino Acid Change	Frequency in the Genome Aggregation Database	CADD score
D190	*DCHS2*	HIGH	exonic	NONSENSE	STOP GAINED	Cga/Tga	p.Arg1343Ter	0.135% rs150179829	38
D041	*FAT2*	LOW	exonic	SILENT	SYNONYMOUS	ttC/ttT	p.Phe1497=	0.00119% rs1024234841	11.57
D965	*DCHS2*	HIGH	exonic	NONSENSE	FRAMESHIFT	aaa/aG-	p.Lys279Serfs*10	0.00%	Not available
D965	*FAT2*	HIGH	exonic	NONSENSE	STOP GAINED	Cga/Tga	p.Arg3476Ter	0.000398% rs377026428	55
D140	*DCHS2*	MODERATE	exonic	MISSENSE	NONSYNONYMOUS CODING	aCa/aAa	p.Thr1328Lys	0.00%	27.5
D831	*FAT2*	MODERATE	exonic	MISSENSE	NONSYNONYMOUS CODING	cGc/cAc	p.Arg1250His	0.00168% rs145224294	34
D205	*FAT2*	MODERATE	exonic	MISSENSE	NONSYNONYMOUS CODING	Gat/Cat	p.Asp2720His	0.00%	23.4

Table 2. Clinical data and pituitary height of patients with variants in *FAT2* and/or *DCHS2*

Patient code	Sex	Age at the time of study (yrs)	Weight at the time of study (kg)	Height at the time of study (cm)	Endocrine disorders	Other findings	Pituitary height (mm)	Normal mean pituitary height (mm ±SD) for age[1]
D190	Male	20.6	N/A	N/A	GHD, TSHD, ACTHD,	micropenis, cryptorchidism	2	5.63 ±1.00
D041	Male	16.4	59.7	162.9	GHD	NR	4	5.10 ±1.17
D965	Male	13.9	55	165	GHD	NR	4	5.10 ±1.17
D140	Female	20.7	45.2	155	GHD	NR	4	6.48 ± 0.95
D831	Male	15.1	46	159.8	GHD, TSHD, partial ACTHD	NR	3	5.10 ±1.17
D205	Male	14.6	54.7	161.8	GHD, TSHD	micropenis, cryptorchidism	4	5.10 ±1.17

[1]Tsunoda et al, Am J Neuroradiol 1997; 18:551–554

GHD: Growth hormone deficiency, TSHD: Thyrotropin hormone deficiency, ACTHD: Adrenocorticotropin hormone deficiency, NR: none reported, N/A: not available.